

Tensile and compressive buckling of columns with shear deformation singularities

S. Caddemi · I. Calìo · F. Cannizzaro

Received: 15 February 2014 / Accepted: 10 May 2014 / Published online: 11 June 2014
© The Author(s) 2014

Abstract Shear deformations in beam-like structures as well as devices allowing deflection discontinuities, besides influencing the compressive buckling, can induce instability in presence of tensile axial loads. In this work a novel study to address both the compressive and the tensile buckling in slender beams in presence of multiple internal sliders endowed with translational springs, that induce deflection discontinuities along the beam axis, is presented. The general exact closed-form solutions is derived as a function of four boundary conditions only, as in the case of homogeneous beam, irrespective on the number of concentrated singularities. The range where the tensile buckling load values are comparable to the compressive counterpart is highlighted. Furthermore, sudden switches from symmetric to anti-symmetric buckling shapes are identified. Finally, for an increasing number of deflection discontinuities an interesting comparison with a uniform column with distributed shear deformations, according to the Timoshenko model, is presented. The latter comparison suggests that elastic internal sliders, which allow transversal deflection discontinuities, can be interpreted as concentrated shear deformations and are addressed to as shear deformation singularities.

Keywords Tensile buckling · Compressive buckling · Displacement discontinuity · Elastic slider · Shear deformations · Column · Singularities

1 Introduction

Occurrence of different types of singularities in structural, mechanical and aerospace engineering components might be the cause of changes in the system properties, of a significant reduction of the operational life and also of failure mechanisms. Efficient analysis tools are required in these cases and, most of all, exact explicit expressions of response parameters might be of great help. In particular, singularities leading to discontinuities of the transversal deflection and the rotation functions of beam-like structures might be adopted to model real phenomena encountered in the common practice and can efficiently model concentrated damage [1–6]. Furthermore, modelling concentrated damage by means of singularities has been shown to be an effective tool to address also the inverse problem of identification of single and multiple cracks [7–10].

With regard to the analysis of the buckling phenomenon that appears in slender columns, the influence of discontinuities of the rotation function only, due to presence of cracks, has been studied

S. Caddemi (✉) · I. Calìo · F. Cannizzaro
Dipartimento Ingegneria Civile e Architettura,
Università di Catania, Via Santa Sofia 64, Catania, Italy
e-mail: scaddemi@dica.unict.it

extensively in the specific literature by using different approaches [11–20]. Very few papers study the buckling phenomenon of columns in presence of discontinuities of the transversal deflection. Those models that include deflection discontinuities due to the presence of a concentrated damage are limited to the analysis of a single crack and address the buckling due to compressive loads only [21, 22].

Besides the compressive buckling phenomenon, it has to be remarked that the occurrence of buckling under the action of tensile axial loads (tensile buckling) has been evidenced by Kelly [23] with regard to highly shear deformable short beams such as the rubber bearing isolators. Relying on the latter work it can be stated that tensile buckling results from accounting for the shear deformability, hence, it can be recovered when the Timoshenko column is considered. Examples of tensile buckling has been studied in damaged columns in presence of single [24] and multiple cracks [25] according to the Timoshenko model. However, the crack model considered in the latter two papers do not account for the presence of any transversal deflection discontinuity.

On the other hand, tensile buckling has been also evidenced, and confirmed by experimental tests, also in concentrated elasticity beam-like structures and in Euler–Bernoulli columns in presence of an internal slider (inducing a transversal displacement discontinuity) as studied in [26, 27]. In the latter works, it has been suggested that the influence of the axial load on the behaviour of columns with internal sliders may provide application to innovative actuators for mechanical wave control.

In view of the numerical and experimental evidence, the following question arises: Is the Euler–Bernoulli column with an internal sliders somehow related to the Timoshenko column?

Starting from this question in this work the case of Euler–Bernoulli column in presence of multiple elastic internal sliders is investigated. The latter internal constraints have not been considered in the last work of the authors [25] where, differently, the tensile buckling phenomenon arose from the distributed shear deformability characterising the Timoshenko beam model.

Internal elastic sliders, inducing transversal deflection discontinuities, are usually studied by imposing suitable continuity and discontinuity conditions at intermediate cross sections, as reported in [26] for the

case of a single slider without transversal spring, leading to an increasing number of integration constants to be determined when multiple singularities have to be accounted for.

In this work the latter classical approach is avoided, the application of the theory of distributions (generalised function) is adopted leading to novel exact explicit expressions of the buckling shape together with an explicit formulation of the buckling load characteristic equation in presence of an arbitrary number of internal sliders. The general solution is obtained as a function of four boundary conditions only, as for the homogeneous beam, irrespective on the number of concentrated singularities.

Both the compressive and the tensile static buckling are addressed by means of the proposed approach. In particular, the range where the tensile buckling load values are comparable to the compressive counterpart is highlighted. Furthermore, sudden switches from symmetric to anti-symmetric buckling shapes are identified both for the compressive and tensile buckling cases. Finally the central question regarding the relation between the Euler–Bernoulli and the Timoshenko columns finds an affirmative answer. The answer is detailed in the work by showing the compressive buckling, and also recovering the tensile buckling, for an increasing number of elastic internal sliders.

2 A model for buckling of Euler–Bernoulli beams with multiple elastic internal sliders

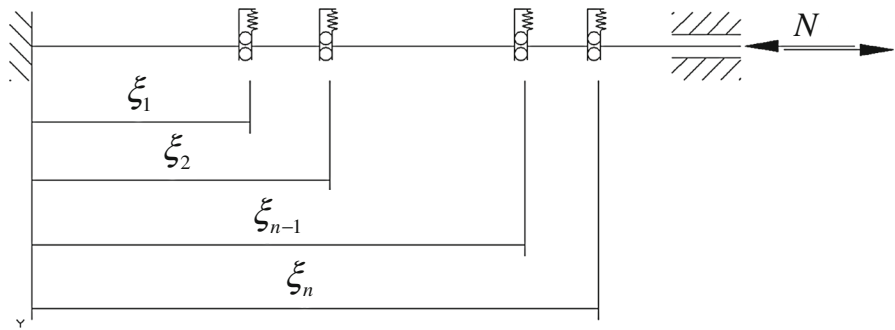
Singularities along the axis of beam-like structures can be promptly modelled by means of distributions. In particular, the correct use of such generalised functions provides the tools to reproduce discontinuities of the response parameters.

In this section a model to deal with deflection discontinuities along the beam axis is presented. In practice the model accounts for the presence of multiple internal sliders endowed with translational springs, as reported in Fig. 1.

The buckling governing equation of Euler–Bernoulli beams in presence of multiple elastic internal sliders, under the action of an axial load, is considered and the exact solution is obtained in explicit form.

Let us consider an Euler–Bernoulli beam with length L and referred to the normalised abscissa

Fig. 1 Euler–Bernoulli column with multiple internal elastic sliders



$0 \leq \xi = x/L \leq 1$. The normalised deflection response function $u(\xi)$ with a single discontinuity $\Delta u(\xi_i)$ at the cross section ξ_i is described over the entire beam length by the following expression $u(\xi) + \Delta u(\xi_i)U(\xi - \xi_i)$, where $U(\xi - \xi_i)$ is the well known Heaviside unit step generalised function. The presence of such deflection discontinuity should be guaranteed in the fourth order buckling governing equation by an additional term that avoids the formulation over different fields and the consequent enforcement of any continuity and discontinuity conditions at ξ_i . Differently from what proposed in [28], a convenient distributional model able to capture such discontinuity in the governing equation requires the introduction of the fourth derivative of the Heaviside function by means of the following term $\Delta u(\xi_i)\delta'''(\xi - \xi_i)$ where $\delta(\xi - \xi_i)$ indicates the Dirac's delta centred at ξ_i and the apex means derivative with respect to the normalised abscissa ξ .

The unknown deflection discontinuity $\Delta u(\xi_i)$ has to be associated to the shear force at ξ_i^- , i.e. at the left of the cross-section where the discontinuity occurs, as follows:

$$\Delta u(\xi_i) = -\lambda_i u'''(\xi_i^-) \tag{1}$$

where λ_i is the normalised translational spring compliance related to the translational spring stiffness K_i as follows: $\lambda_i = \frac{EI}{K_i} \frac{1}{L^3}$ with EI the flexural stiffness of the uniform beam.

The behaviour of a uniform Euler–Bernoulli beam subjected to a constant axial force N (column), in presence of n along axis internal sliders, is hence governed by the following differential equation:

$$u^{IV}(\xi) \pm \sigma^2 u''(\xi) = \sum_{i=1}^n \Delta u(\xi_i) \delta'''(\xi - \xi_i) \tag{2}$$

where the axial load parameter $\sigma^2 = \frac{NL^2}{EI}$ has been introduced. The term $\pm \sigma^2 u''(\xi)$ accounts for the

influence of the axial force in the buckling equation where the upper or lower sign applies to the case of compressive or tensile axial load, respectively.

The solution of Eq. (2), characterised by the unknown singular term on the right hand side, is pursued by means of application of the Laplace Transform as follows:

$$u(s) = \frac{1}{s^2(s^2 \pm \sigma^2)} \times \left[s(s^2 \pm \sigma^2)u(0) + (s^2 \pm \sigma^2)u'(0) + s u''(0) + u'''(0) + \sum_{i=1}^n s^3 e^{-s \xi_i} \Delta u(\xi_i) \right] \tag{3}$$

where the variable s represents the complex frequency introduced to perform the Laplace transform. The inverse Laplace transform of Eq. (3) provides the following expression for the deflection function $u(\xi)$:

$$u(\xi) = h_1^\pm(\xi)u(0) + h_2^\pm(\xi)u'(0) + h_3^\pm(\xi)u''(0) + h_4^\pm(\xi)u'''(0) + \sum_{i=1}^n \bar{h}_i^\pm(\xi)\Delta u(\xi_i) \tag{4}$$

where the functions $h_1^\pm(\xi), h_2^\pm(\xi), h_3^\pm(\xi), h_4^\pm(\xi), \bar{h}_i^\pm(\xi)$, apex + for the compressive and apex – for the tensile axial load, are defined by the following expressions:

$$\begin{aligned} h_1^+(\xi) &= 1 & h_1^-(\xi) &= 1 \\ h_2^+(\xi) &= \xi & h_2^-(\xi) &= \xi \\ h_3^+(\xi) &= \frac{1 - \cos \sigma \xi}{\sigma^2} & h_3^-(\xi) &= \frac{\cosh \sigma \xi - 1}{\sigma^2} \\ h_4^+(\xi) &= \frac{1}{\sigma^3}(\sigma \xi - \sin \sigma \xi) & h_4^-(\xi) &= \frac{1}{\sigma^3}(\sinh \sigma \xi - \sigma \xi) \\ \bar{h}_i^+(\xi) &= \cos \sigma(\xi - \xi_i)U(\xi - \xi_i) & \bar{h}_i^-(\xi) &= \cosh \sigma(\xi - \xi_i)U(\xi - \xi_i) \end{aligned} \tag{5}$$

The key passages leading to Eq. (4) by means of the Laplace transform and the inverse Laplace transform

are reported in [Appendix](#) for convenience. On the other hand, the definition of the successive derivatives of distributions and the related rules can be found in [29–31].

Equation (4) does not provide an explicit expression for the deflection function $u(\xi)$ since it depends on the unknown discontinuity $\Delta u(\xi_i)$ at ξ_i that requires, in view of Eq. (1), the evaluation of the third derivative of the deflection function $u'''(\xi_i^-)$ at the same cross section.

Substitution of Eq. (1) into Eq. (4), and evaluation of the third derivative, provides the following expression for $u'''(\xi_i^-)$:

$$\begin{aligned} u'''(\xi_i^-) &= h_1^{\pm''' }(\xi_i^-)u(0) + h_2^{\pm''' }(\xi_i^-)u'(0) \\ &\quad + h_3^{\pm''' }(\xi_i^-)u''(0) + h_4^{\pm''' }(\xi_i^-)u'''(0) \\ &\quad - \sum_{k=1}^{i-1} \bar{h}_k^{\pm''' }(\xi_i^-)\lambda_i u'''(\xi_k^-) \end{aligned} \quad (6)$$

The third derivative of the deflection function at ξ_i^- , given by Eq. (6), can be transformed, after some algebra, in explicit form as follows:

$$\begin{aligned} u'''(\xi_i^-) &= g_1^{\pm}(\xi_i^-)u(0) + g_2^{\pm}(\xi_i^-)u'(0) \\ &\quad + g_3^{\pm}(\xi_i^-)u''(0) + g_4^{\pm}(\xi_i^-)u'''(0) \end{aligned} \quad (7)$$

where the terms $g_j^+(\xi_i^-)$ and $g_j^-(\xi_i^-)$, $j = 1, \dots, 4$, to be adopted for the compressive and the tensile axial load, respectively, are defined by the following expressions:

$$\begin{aligned} g_j^{\pm}(\xi_i^-) &= h_j^{\pm''' }(\xi_i^-) - \sum_{k=1}^{i-1} \bar{h}_k^{\pm''' }(\xi_i^-)\lambda_k g_j^{\pm}(\xi_k^-), \quad (8) \\ j &= 1, \dots, 4 \end{aligned}$$

Substitution of Eq. (7) into Eq. (4), in view of Eq. (1), provides the following explicit expression of the deflection function assumed by the column in its buckled configuration:

$$\begin{aligned} u(\xi) &= f_1^{\pm}(\xi)u(0) + f_2^{\pm}(\xi)u'(0) + f_3^{\pm}(\xi)u''(0) \\ &\quad + f_4^{\pm}(\xi)u'''(0) \end{aligned} \quad (9)$$

where

$$f_j^{\pm}(\xi) = h_j^{\pm}(\xi) - \sum_{i=1}^n \bar{h}_i^{\pm}(\xi)\lambda_i g_j^{\pm}(\xi_i^-), \quad j = 1, \dots, 4 \quad (10)$$

Equation (9) represents a novel achievement since, to the best of the authors' knowledge, explicit solution

of the static, both compressive and tensile, buckling problem of the Euler–Bernoulli beam in presence of multiple elastic internal sliders, allowing a convenient parametric analysis, has never been presented in the literature. Equation (9) requires the enforcement of four boundary conditions in order to obtain the buckling load and the relevant buckling shape. In particular the case of clamped–clamped column with single and multiple elastic internal sliders will be extensively treated in Sect. 4.

3 The moment discontinuities at the internal sliders

The proposed model based on the use of distributions, discussed in the previous section, implies that the discontinuity conditions due to the elastic internal sliders are embedded in the explicit closed form solution of the column. Precisely, at cross-sections at abscissae ξ_i , the column undergoes a transversal deflection discontinuity that has to be considered in the deformed configuration to study the stability problem. Due to the presence of the axial load the mentioned deflection discontinuity implies a discontinuity of the bending moment as depicted in Fig. 2.

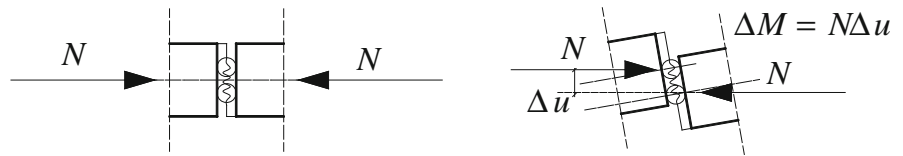
When classical approaches, requiring the enforcement of additional conditions at the discontinuity cross-sections, are adopted, the latter bending moment discontinuity has to be accounted for explicitly by imposing the following condition at the discontinuity cross-sections:

$$u''(\xi_i^+) - u''(\xi_i^-) = \pm \sigma^2 [u(\xi_i^+) - u(\xi_i^-)], \quad (11) \\ i = 1, \dots, n$$

In addition, at ξ_i , the rotation and shear force continuity has to be enforced as follows $u'(\xi_i^+) = u'(\xi_i^-)$, $u'''(\xi_i^+) = u'''(\xi_i^-)$ together with the deflection discontinuity $u(\xi_i^+) - u(\xi_i^-) = -\lambda_i u'''(\xi_i^-)$.

The explicit closed form solution presented in Eqs. (9), (10) holds for any number of deflection discontinuities and requires the evaluation of four boundary conditions only. On the contrary, classical approaches do not provide explicit closed form solutions since require four additional boundary conditions for each singularity. Hence the adoption of Eqs. (9), (10) is recommended for columns with multiple singularities. The latter statement is proved in the next section

Fig. 2 Bending moment discontinuity due to the axial load at a cross-section with an internal slider



where explicit form of the buckling load characteristic equation is derived for the clamped–clamped column.

4 The case of a clamped–clamped column with internal elastic sliders subjected to an axial compressive/tensile load

The adoption of classical approaches to the problem at hand would require enforcement of continuity conditions at each cross-section endowed with an internal slider. As a consequence, no explicit solution of the governing equation has been previously presented. The consequent buckling load equation would be obtained by a matrix whose order increases with the number of sliders. On the contrary, the passages presented from Eqs. (3) to (10) lead to a solution in terms of four integration constants only, as also required by columns without any singularity. Whatever the number of sliders, four conditions only have to be enforced to derive the buckling load equation.

The closed form solution presented in Sect. 2 is here exploited to study the case of a clamped–clamped column in presence of multiple elastic internal sliders. The buckling load characteristic equation is obtained by the following boundary conditions for the case at hand:

$$u(0) = 0; \quad u'(0) = 0; \quad u(1) = 0; \quad u'(1) = 0 \tag{12}$$

In view of the closed-form solution provided by Eqs. (9), (10), enforcement of the boundary conditions in Eq. (12) leads to:

$$G(\sigma) = \begin{bmatrix} f_3^\pm(1) & f_4^\pm(1) \\ f_3^{\pm'}(1) & f_4^{\pm'}(1) \end{bmatrix} \begin{bmatrix} u''(0) \\ u'''(0) \end{bmatrix} = \begin{bmatrix} 0 \\ 0 \end{bmatrix} \tag{13}$$

where, in view of Eqs. (5), (10), the terms $f_3^\pm(1)$, $f_4^\pm(1)$, $f_3^{\pm'}(1)$, $f_4^{\pm'}(1)$ are given the following compact form:

$$\begin{aligned} f_3^\pm(1) &= \pm \frac{1 - c^\pm}{\sigma^2} + \sum_{i=1}^n C_i^\pm \lambda_i g_3^\pm(\xi_i^-), \\ f_4^\pm(1) &= \pm \frac{1}{\sigma^3} (\sigma - s^\pm) + \sum_{i=1}^n C_i^\pm \lambda_i g_4^\pm(\xi_i^-), \\ f_3^{\pm'}(1) &= \frac{s^\pm}{\sigma} \mp \sum_{i=1}^n \sigma S_i^\pm \lambda_i g_3^\pm(\xi_i^-), \\ f_4^{\pm'}(1) &= \pm \frac{1 - c^\pm}{\sigma^2} \mp \sum_{i=1}^n \sigma S_i^\pm \lambda_i g_4^\pm(\xi_i^-) \end{aligned} \tag{14}$$

where the following positions have been introduced:

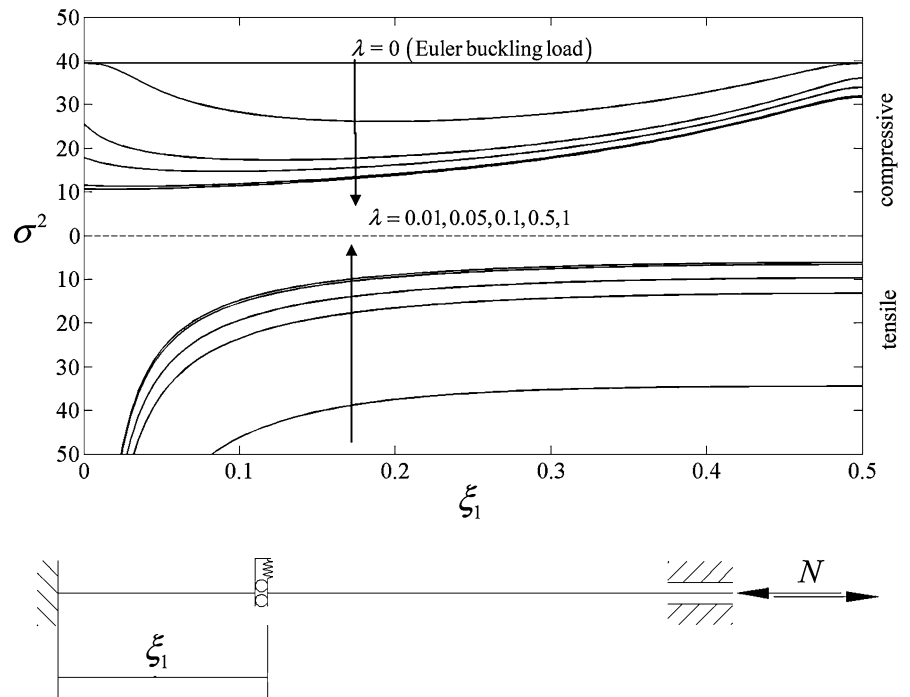
$$\begin{aligned} s^+ &= \sin \sigma; \quad c^+ = \cos \sigma; \quad S_i^+ = \sin \sigma(1 - \xi_i); \\ C_i^+ &= \cos \sigma(1 - \xi_i); \quad s^- = \sinh \sigma; \quad c^- = \cosh \sigma; \\ S_i^- &= \sinh \sigma(1 - \xi_i); \quad C_i^- = \cosh \sigma(1 - \xi_i) \end{aligned} \tag{15}$$

and the terms $g_3^\pm(\xi_i^-)$, $g_4^\pm(\xi_i^-)$, are given, in view of Eqs. (5), (8), as follows:

$$\begin{aligned} g_3^+(\xi_i^-) &= -\sigma \sin \sigma \xi_i - \sum_{k=1}^{i-1} \sigma^3 \sin \sigma(\xi_i - \xi_k) \lambda_k g_3^+(\xi_k^-) \\ g_3^-(\xi_i^-) &= \sigma \sinh \sigma \xi_i - \sum_{k=1}^{i-1} \sigma^3 \sinh \sigma(\xi_i - \xi_k) \lambda_k g_3^-(\xi_k^-) \\ g_4^+(\xi_i^-) &= \cos \sigma \xi_i - \sum_{k=1}^{i-1} \sigma^3 \sin \sigma(\xi_i - \xi_k) \lambda_k g_4^+(\xi_k^-) \\ g_4^-(\xi_i^-) &= \cosh \sigma \xi_i - \sum_{k=1}^{i-1} \sigma^3 \sinh \sigma(\xi_i - \xi_k) \lambda_k g_4^-(\xi_k^-) \end{aligned} \tag{16}$$

The buckling load characteristic equation is obtained by setting equal to zero the second-order determinant of the system of Eqs. (13), expressed in terms of the axial load parameter σ , in view of Eq. (14), as follows:

Fig. 3 Buckling load parameter σ^2 versus the slider position ξ_1 for a clamped–clamped column with a single elastic slider for given values of the compliance parameter λ



$$\begin{aligned}
 & \left[\pm \frac{1 - c^\pm}{\sigma^2} + \sum_{i=1}^n C_i^\pm \lambda i f_3^{\pm''' }(\xi_i) \right] \\
 & \times \left[\pm \frac{1 - c^\pm}{\sigma^2} \mp \sum_{i=1}^n \sigma S_i^\pm \lambda i f_4^{\pm''' }(\xi_i) \right] \\
 & - \left[\pm \frac{1}{\sigma^3} (\sigma - s^\pm) + \sum_{i=1}^n C_i^\pm \lambda i f_4^{\pm''' }(\xi_i) \right] \\
 & \times \left[\frac{s^\pm}{\sigma} \mp \sum_{i=1}^n \sigma S_i^\pm \lambda i f_3^{\pm''' }(\xi_i) \right] = 0
 \end{aligned} \tag{17}$$

Equation (17) is the sought explicit form for the buckling load characteristic equation where the upper sign and the upper apex have to be adopted for the compressive axial load, while the lower sign and the lower apex for the tensile axial load.

Once the compressive/tensile critical values of the axial load parameter $\sigma^2 = \frac{NL^2}{EI}$ are obtained, by solving Eq. (17), the critical compressive/tensile buckling shapes are obtained by determining the two unknown boundary values $u''(0)$, $u'''(0)$, by solving the system in Eq. (13), and substituting in the solution (9).

5 Numerical applications

The proposed explicit closed form expressions presented in the previous sections are here exploited to investigate on the influence of single and multiple elastic internal sliders on the column buckling with regard to the position, spatial distribution and the compliance of the elastic slider.

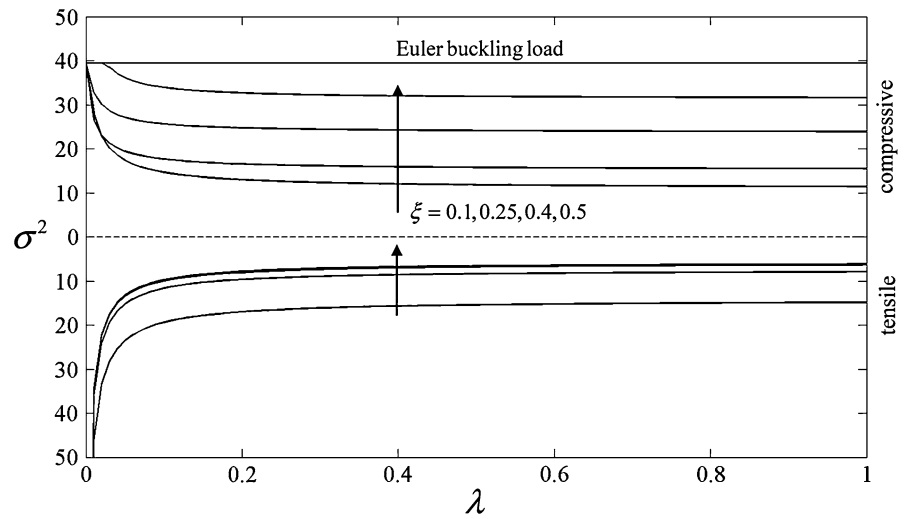
The detailed buckling behaviour will be discussed both for the compressive and the tensile case and a comparative analysis is also presented in this section.

5.1 A single elastic slider

The case of a single slider is considered in Fig. 3 where the buckling load values, in terms of the $\sigma^2 = \frac{NL^2}{EI}$ parameter, versus the slider position ξ_1 is reported. In Fig. 3 the upward values of σ^2 refer to the compressive buckling load, the downward values to the tensile load.

Besides the horizontal line at $\sigma^2 = 4\pi^2$, representing the Euler compressive buckling load of the homogeneous column without slider, five curves have been reported for different values of compliance

Fig. 4 Buckling load parameter σ^2 versus the compliance parameter λ for a clamped–clamped column with a single elastic slider for given values of the slider position ξ_1



$\lambda = 0.01, 0.05, 0.1, 0.5, 1$. With regard to the compressive buckling load values, different behaviours are shown as the compliance λ increases. A detailed description is as follows. When the slider is adjacent either to the clamped end ($\xi_1 = 0$) or to the middle cross-section ($\xi_1 = 0.5$), low values of λ do not alter the buckling load with respect to the homogeneous column. Furthermore, for low values of the compliance parameter λ , the maximum decrement of the compressive buckling load is attained at an intermediate position of the slider. On the other hand, as the compliance λ increases the buckling load value diminishes when the slider is next to the clamped end or the middle cross-section. Finally, for high values of the compliance λ the compressive buckling load obtained for the slider at the clamped end represents the absolute minimum.

With regard to the tensile case it has to be preliminarily remarked that no buckling phenomenon occurs in the homogeneous column (i.e. without any slider) or when the slider is located at the clamped end. Then, Fig. 3 shows that, as the slider moves from the clamped end, the tensile buckling phenomenon appears. Precisely, the tensile buckling load decreases as the abscissa ξ_1 increases from 0 up to 0.5. The minimum value of the tensile buckling load is attained at the middle cross-section $\xi_1 = 0.5$. It has to be remarked that, except for the range $0 \leq \xi_1 < 0.1$, the values of the tensile buckling load are comparable to the compressive buckling load ones.

Furthermore, it has to be noted that, when the slider is located at the middle cross-section and for the elastic compliance parameter $\lambda \rightarrow \infty$, the values of compressive and tensile buckling load $\sigma^2 = 31.3526$ and $\sigma^2 = 5.7993$, respectively, obtained in the literature by Zaccaria et al. [26] for a slider, in absence of any translational elastic spring, are recovered.

In order to present a wider perspective regarding the influence of the slider compliance, in Fig. 4 the buckling load is plotted against the compliance parameter λ for different positions $\xi_1 = 0.1, 0.25, 0.4, 0.5$ of the internal slider. For all cases, as the compliance parameter λ increases, the buckling load undergoes a rapid decrement and tends asymptotically to a constant value. Furthermore, for the compressive case the buckling load increases as the slider moves towards the middle cross-section (except for very small values of the compliance parameter) while for the tensile case the buckling load decreases.

The buckling shapes for the compressive and the tensile cases are depicted in Figs. 5 and 6, respectively, for the slider at the middle cross-section with a high value $\lambda = 10$ of the elastic compliance. As already enhanced in the literature [26] for the case of a single slider without the translational elastic spring (i.e. $\lambda \rightarrow \infty$) compressive and tensile buckling occur with different shapes as it is clearly shown by a comparison of Figs. 5a and 6a. Furthermore, the buckling shape in terms of rotation function undergoes

Fig. 5 Compressive buckling shape functions clamped–clamped column with a single slider ($\lambda = 10$, $\xi_j = 0.5$) in terms of **a** displacement and rotation and **b** bending moment and shear force

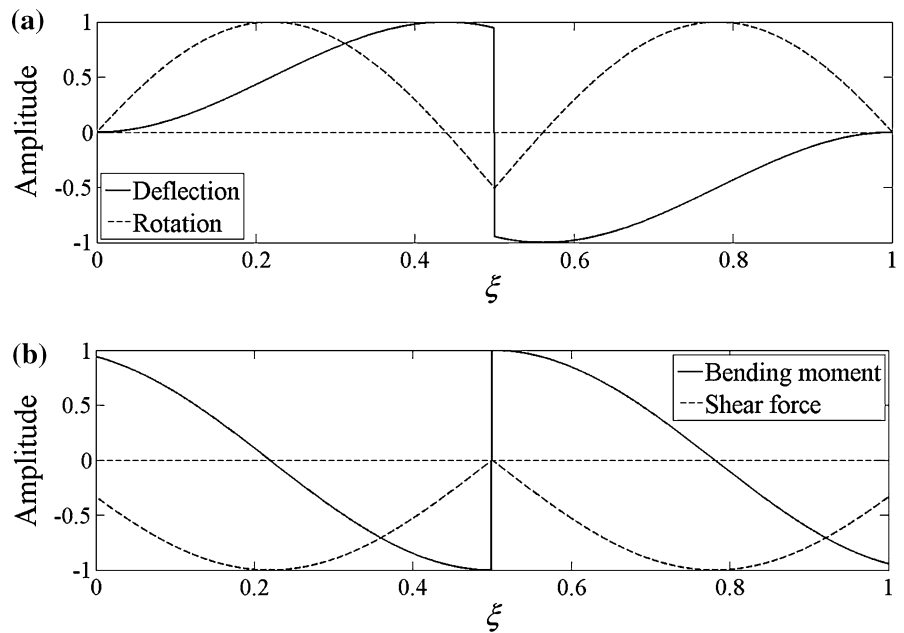
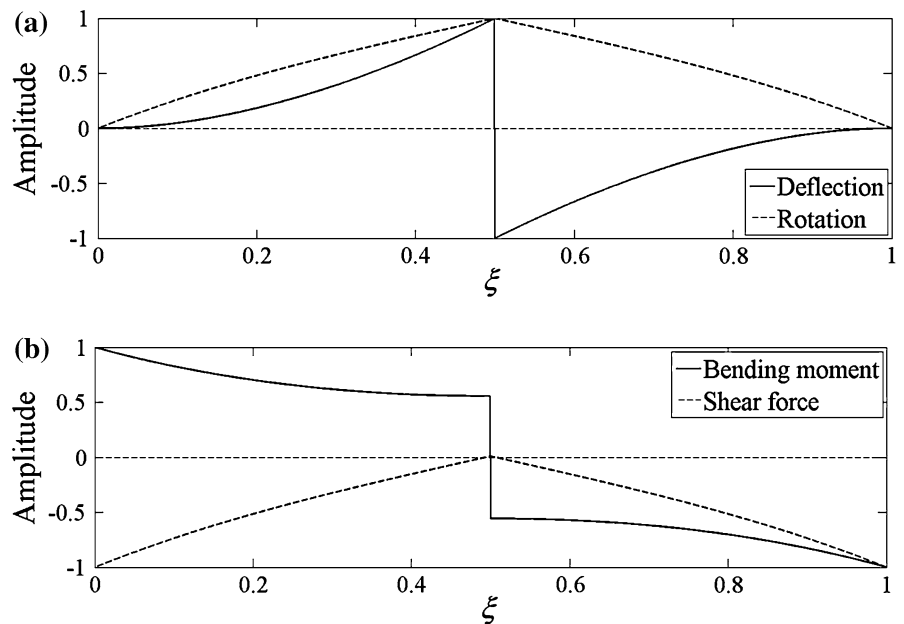


Fig. 6 Tensile buckling shape functions clamped–clamped column with a single slider ($\lambda = 10$, $\xi_j = 0.5$) in terms of **a** displacement and rotation and **b** bending moment and shear force



a change of sign in the compressive case (Fig. 5b) that is not encountered for the tensile case (Fig. 6b). Moreover, the displacement and bending moment discontinuities appropriately captured by the adopted model, as clearly outlined in Sect. 3, appear for both compressive (Fig. 5a, c) and tensile (Fig. 6a, c) buckling. Buckling shapes expressed in terms of rotation (Figs. 5b, 6b) and shear force (Figs. 5d, 6d) are continuous but undergo first order discontinuities.

The shear force is close to zero at the middle cross-section in view of the high value assumed for the elastic compliance.

5.2 Two elastic sliders at symmetric positions

The presented model allows to analyse the case of two internal sliders with elastic springs without the introduction of any additional condition at the discontinuity

Fig. 7 Buckling load parameter σ^2 versus the slider position ξ_1 for a clamped–clamped column with two symmetric elastic sliders for given values of the compliance parameter λ

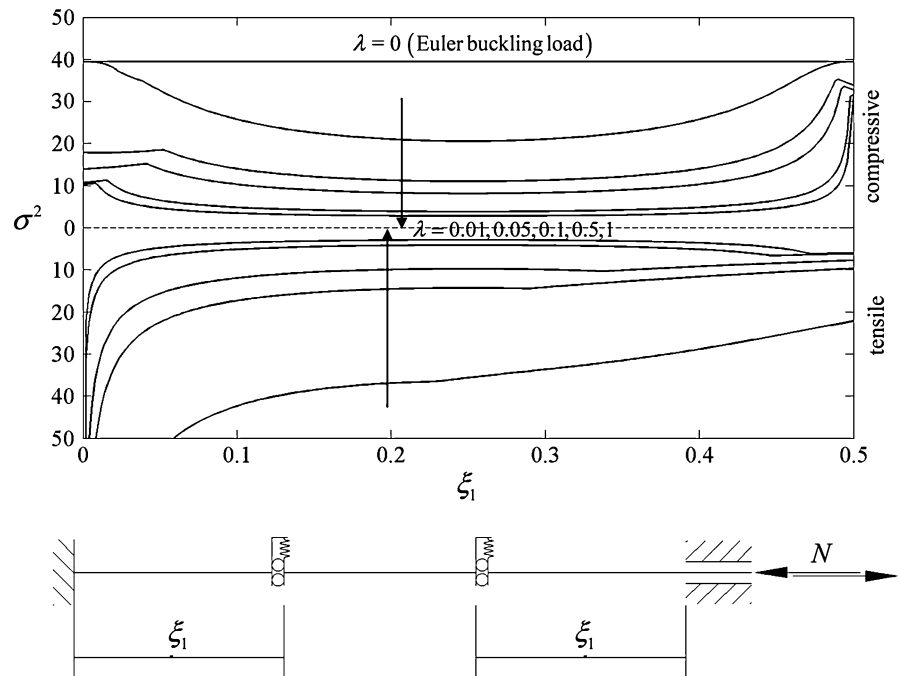
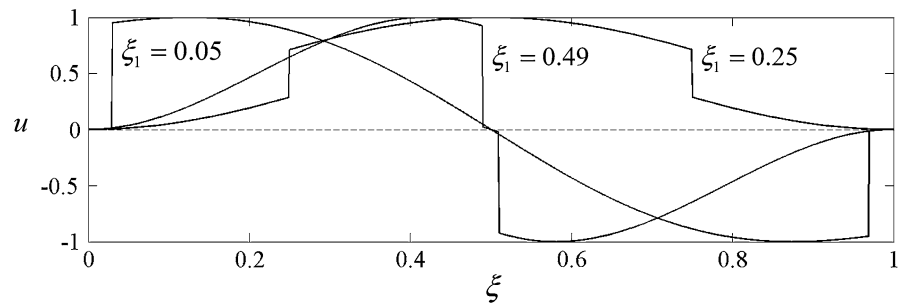


Fig. 8 Buckling shapes for a clamped–clamped column in compression for different positions of two symmetric sliders ($\lambda = 0.05$)



cross-section. As a matter of example the two sliders are here considered endowed with the same elastic compliance and placed at symmetric positions along the column axis identified by the distance from the clamped ends denoted as ξ_1 .

In Fig. 7 the buckling load parameter σ^2 versus the slider position parameter ξ_1 is reported.

It can be noted that, both for compressive and tensile load, the buckling load decreases monotonically for a fixed position ξ_1 of the internal sliders as the spring compliance increases. On the contrary, Fig. 7 shows that, for a fixed value of the spring compliance, the buckling load undergoes a non monotonic behaviour. The latter non monotonic behaviour is due to the presence of corners in the buckling load curves that correspond to sudden switches to different buckling

shapes. Precisely, for the compressive case two corners for each curve are shown in Fig. 7 denoting three different regions of the slider positions where buckling occurs with different mode shapes. The first region, where both sliders are adjacent to the clamped end, and the third region, identified by both sliders next to the middle cross-section, correspond to compressive buckling occurring with anti-symmetric shapes as depicted in Fig. 8a, c for $\xi_1 = 0.05$ and $\xi_1 = 0.49$, respectively. The second, more extended, region comprising intermediate positions of the sliders, induces compressive buckling with the symmetric shape as reported in Fig. 8b for the case $\xi_1 = 0.25$.

For the tensile case, one corner only is encountered in Fig. 7 for each curve. This corner point separates positions of the two sliders inducing symmetric tensile

Fig. 9 Buckling shapes for a clamped–clamped column in tension for different positions of two symmetric sliders ($\lambda = 0.05$)

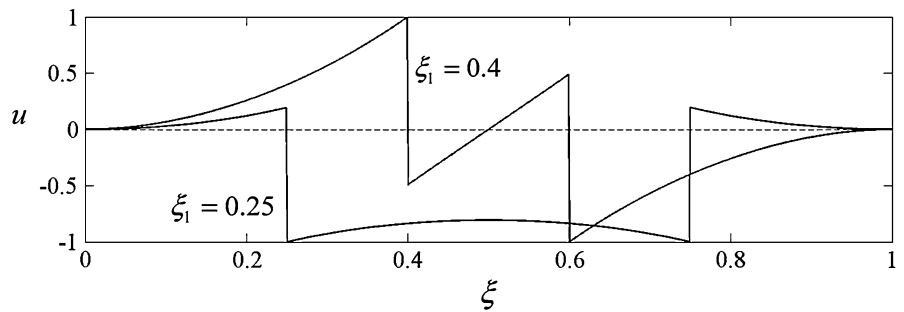
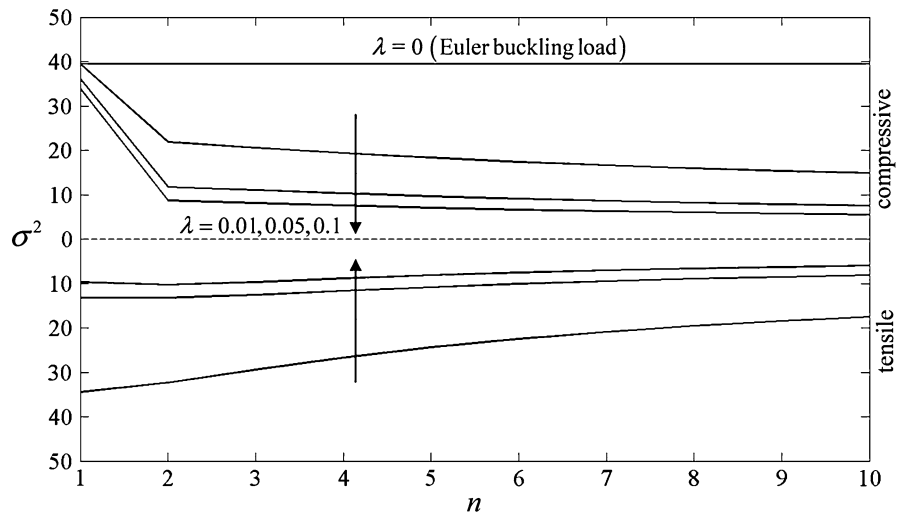


Fig. 10 Buckling load parameter σ^2 versus the number of sliders for a clamped–clamped column for given values of the compliance parameter λ



buckling shapes from anti-symmetric buckling shapes. Two examples of the latter cases are depicted in Fig. 9a, b where the symmetric and anti-symmetric buckling shapes are reported for the tensile load for $\xi_1 = 0.25$ and $\xi_1 = 0.4$, respectively. In addition, Fig. 7 shows that the mentioned corner for tensile buckling curves moves toward the middle cross-section as the elastic compliance parameter increases. As a result the region of the slider positions inducing a symmetric tensile buckling shape becomes wider as the elastic springs stiffness decreases. Under the latter circumstance the anti-symmetric shape, somehow resembling that obtained for the single slider, occurs only when the two sliders approach the middle cross-section.

5.3 Multiple elastic sliders evenly distributed along the axis

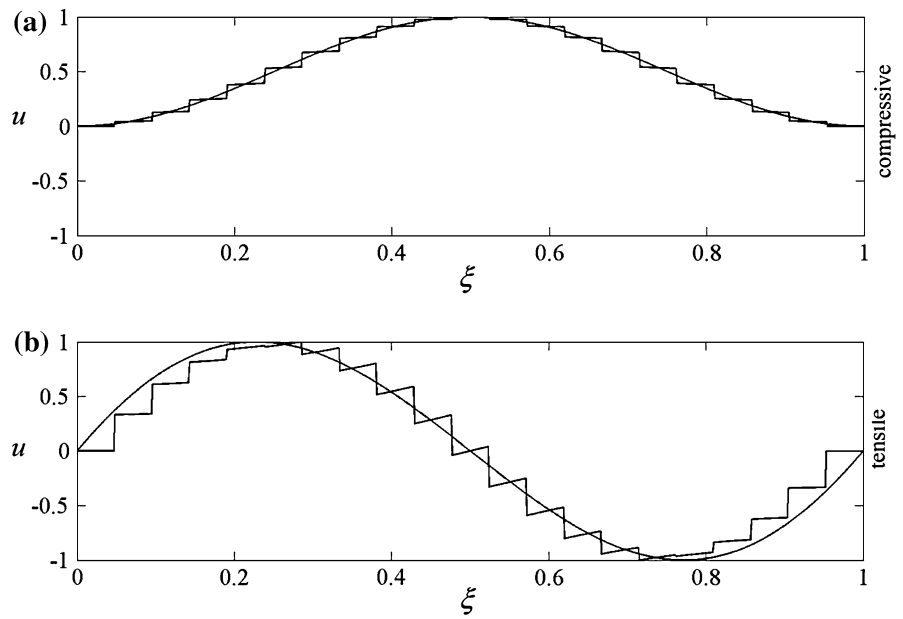
The proposed closed form solution allows a straight treatment of buckling of columns with multiple singularities due to elastic sliders that are here

considered, as a matter of example, placed at constant intervals along the axis. The case of the Euler–Bernoulli column with multiple elastic sliders is the natural evolution of the Euler–Bernoulli column with a single internal slider without elastic spring studied in [26].

In particular, in Fig. 10 the buckling load parameter σ^2 versus the number n of sliders is reported. Inspection of Fig. 10 reveals that a rapid decrement of the compressive buckling is shown from a single to a double slider; on the other hand, as the number of sliders increases, the decrement of the compressive buckling load attenuates. The same rapid decrement with the occurrence of the second slider is not encountered in the tensile case. Furthermore, Fig. 10 shows that the tensile buckling load becomes less sensitive to the number of sliders as the elastic compliance parameter λ increases.

Finally, in Fig. 11 the deflection buckling shapes are presented for $n = 20$ sliders evenly distributed along the column axis and with the same compliance

Fig. 11 Buckling shapes for a clamped–clamped column with 20 evenly distributed sliders with $\lambda = 0.1$ (discontinuous lines) and for the uniform Timoshenko column with shear stiffness parameter $br^2 = 0.5$ (continuous lines): **a** compressive and **b** tensile buckling



parameter $\lambda = 0.1$, both for the compressive and the tensile case.

At this stage it is worth mentioning that the tensile buckling behaviour in the considered Euler–Bernoulli column arose from the presence of multiple elastic sliders. On the other hand, since the tensile buckling has been also encountered in columns with distributed shear deformation, consistently to the classical Timoshenko model, a comparison between the two models deserves attention.

In the classical Timoshenko column the compressive buckling occurs under a symmetric buckling shape while the tensile buckling under an anti-symmetric buckling shape as shown in [25]. On the other hand, for the Euler–Bernoulli column with multiple elastic sliders, it can be observed in Fig. 11 that the compressive and tensile buckling occur with a symmetric and an anti-symmetric shape, respectively, that are compared with buckling shapes of the Timoshenko column where the normalised shear stiffness parameter $br^2 = \frac{EI}{G_o A_o} L^2 = 0.5$ (with $G_o A_o$ the column shear stiffness) has been adopted.

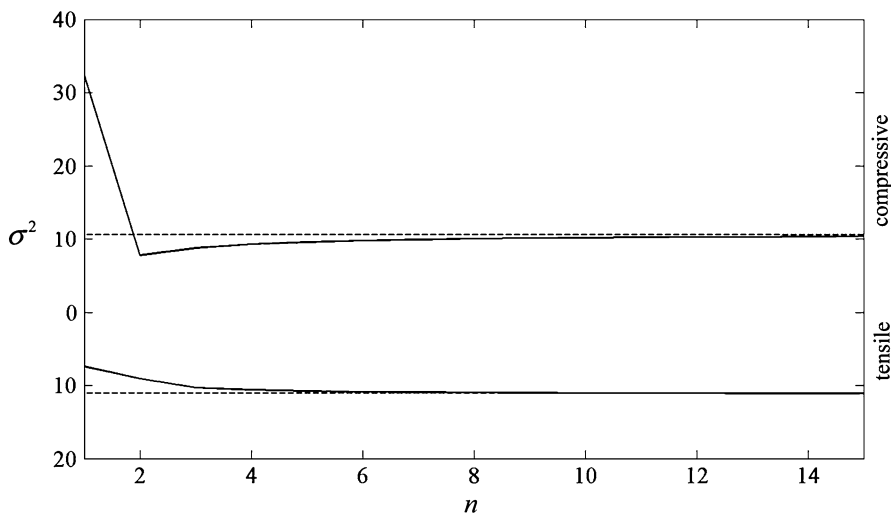
A final comparison between the Euler–Bernoulli column with multiple elastic sliders and the homogeneous Timoshenko column is provided in Fig. 12. The buckling load values $\sigma^2 = 10.61064$ (compressive) and $\sigma^2 = 11.066$ (tensile) of the Timoshenko column with $br^2 = 0.4 \pi^2$ obtained in [25] are

compared with the Euler–Bernoulli beam with an increasing number n of internal elastic sliders. To this aim, it has to be pointed out that the normalised shear stiffness parameter of the Timoshenko column can be related to the compliance of the elastic sliders as follows $br^2 = \frac{1}{n\lambda}$. Inspection of Fig. 12 reveals that the buckling load of the uniform Timoshenko column with equivalent shear stiffness parameter $br^2 = 0.4 \pi^2$ is recovered as the number of elastic sliders in the Euler–Bernoulli column increases.

It can be concluded that, although the Euler–Bernoulli model is not characterised by shearing strain and angular distortion, proper of the Timoshenko model, multiple elastic internal sliders are able to reproduce the effect of the distributed shear deformation of the Timoshenko column. The Euler–Bernoulli column with multiple elastic sliders might, hence, be considered somehow as a discrete counterpart of a column with distributed shear deformation according to the classical Timoshenko model.

Shear deformations, implying angular distortion between the cross-section and the beam axis, in a beam segment produce a difference of transversal displacement between the two extreme cross-sections of the segment while an internal slider induces a difference of transversal displacement concentrated at a cross-section (discontinuity).

Fig. 12 Buckling load parameter σ^2 vs the number of sliders for a clamped–clamped Euler–Bernoulli column (continuous lines) and for the uniform Timoshenko column (dashed lines) with $br^2 = 0.4 \pi^2$



It can hence be stated that transversal deflection discontinuities can be addressed to as “*shear deformation singularities*”, even though applied to the Euler–Bernoulli model, in the sense that has been above clarified, i.e. shear deformations occurring in an infinitesimal beam segment.

6 Closure

In this work tensile and compressive buckling of the Euler–Bernoulli column in presence of multiple elastic sliders, interpreted as shear deformation singularities, has been investigated. The presented model, relying on the use of distributions, allowed the formulation of a novel exact solution in explicit form.

The presented study is concluded by addressing the following question that has been posed in the Introduction: “Is the Euler–Bernoulli column with an internal slider somehow related to the Timoshenko column?”.

On the basis of the presented results, it can be stated that the Euler–Bernoulli column with shear deformation singularities can be considered as the discrete counterpart of the uniform Timoshenko column and its accuracy in terms of compressive/tensile buckling load depends on the number of singularities considered in the model.

The presented model, showing static bifurcation of the field equations due to the presence of internal translational springs, reproduces somehow the constitutive bifurcation usually occurring under yielding or else in materials with a high shear deformability in the elastic regime.

Appendix

In this appendix, starting from the governing equation of the Euler–Bernoulli column in presence of multiple deflection discontinuities, the key passages leading to the expression of the deflection function in the buckled configuration in Eq. (4), together with the definition of the functions $h_1^\pm(\xi), h_2^\pm(\xi), h_3^\pm(\xi), h_4^\pm(\xi), \bar{h}_i^\pm(\xi)$ reported in Eq. (5), are presented in detail.

Precisely, application of the Laplace transform to Eq. (2) leads to:

$$\begin{aligned}
 & s^4 u(s) - s^3 u(0) - s^2 u'(0) - s u''(0) - u'''(0) \\
 & \pm \sigma^2 s^2 u(s) \mp \sigma^2 s u(0) \mp \sigma^2 u'(0) \\
 & = \sum_{i=1}^n s^3 e^{-s x_i} \Delta u(\xi_i)
 \end{aligned} \tag{18}$$

where $u(s) = \mathcal{L}\{u(\xi)\}$ is the Laplace transform of the deflection function $u(\xi)$, the variable s being the complex frequency variable introduced to perform the Laplace transform. Solving Eq. (18) in terms of $u(s)$ leads to:

$$\begin{aligned}
 u(s) &= \frac{1}{s} u(0) + \frac{1}{s^2} u'(0) + \frac{1}{s(s^2 \pm \sigma^2)} u''(0) \\
 &+ \frac{1}{s^2(s^2 \pm \sigma^2)} u'''(0) \\
 &+ \frac{1}{s^2(s^2 \pm \sigma^2)} \sum_{i=1}^n s^3 e^{-s x_i} \Delta u(\xi_i)
 \end{aligned} \tag{19}$$

The inverse Laplace transform of Eq. (19) provides the expression of the deflection function $u(\xi) =$

$\mathcal{L}^{-1}\{u(s)\}$ in the original spatial normalised abscissa ξ . However, application of the inverse Laplace transform provides two different expressions for the deflection function $u(\xi)$ according to the sign of the buckling parameter σ^2 as follows:

$$u(\xi) = u(0) + u'(0) + \frac{u''(0)}{\sigma^2} [1 - \cos \sigma \xi] + \frac{u'''(0)}{\sigma^3} [\sigma \xi - \sin \sigma \xi] + \sum_{i=1}^n \Delta u(\xi_i) \cos \sigma(\xi - \xi_i) U(\xi - \xi_i) \tag{20}$$

when the case of compressive axial load is considered in Eq. (19), and:

$$u(\xi) = u(0) + u'(0) + \frac{u''(0)}{\sigma^2} [\cosh \sigma \xi - 1] + \frac{u'''(0)}{\sigma^3} [\sinh \sigma \xi - \sigma \xi] + \sum_{i=1}^n \Delta u(\xi_i) \cosh \sigma(\xi - \xi_i) U(\xi - \xi_i) \tag{21}$$

if, otherwise, the case of tensile axial load, for the buckling parameter σ^2 appearing in Eq. (19), is considered.

Equations (20) and (21) are equivalent to the compact form reported in Eq. (4) in the main text if the definitions proposed in Eq. (5) for the functions $h_1^\pm(\xi), h_2^\pm(\xi), h_3^\pm(\xi), h_4^\pm(\xi), h_7^\pm(\xi)$ are accounted for.

References

1. Freund LB, Hermann G (1976) Dynamic fracture of a beam or plate in plane bending. *J Appl Mech* 76:112–116
2. Okamura H, Watanabe K, Takano T (1973) Applications of compliance concept in fracture mechanics. In: Kaufman JG (ed) *Progress in flaw growth and fracture toughness testing*, vol 536. American Society for Testing and Materials, Philadelphia, pp 423–438
3. Tharp T (1987) A finite element for edge-cracked beam columns. *Int J Numer Method Eng* 24:1941–1950
4. Christides S, Barr ADS (1984) One-dimensional theory of cracked Bernoulli–Euler beams. *Int J Mech Sci* 26(11/12): 639–648
5. Ostachowicz WM, Krawczuk C (1991) Analysis of the effect of cracks on the natural frequencies of a cantilever beam. *J Sound Vib* 150(2):191–201

6. Caddemi S, Caliò I (2009) Exact closed-form solution for the vibration modes of the Euler–Bernoulli beam with multiple open cracks. *J Sound Vib* 327:473–489
7. Morassi A (2001) Identification of a crack in a rod based on changes in a pair of natural frequencies. *J Sound Vib* 242: 577–596
8. Cerri MN, Vestroni F (2000) Detection of damage in beams subjected to diffused cracking. *J Sound Vib* 234:259–276
9. Cerri MN, Dilena M, Ruta G (2008) Vibration and damage detection in undamaged and cracked circular arches: experimental and analytical results. *J Sound Vib* 314:83–94
10. Caddemi S, Caliò I (2014) Exact reconstruction of multiple concentrated damages on beams. *Acta Mech*. doi:10.1007/s00707-014-1105-5
11. Liebowitz H, Vanderveldt H, Harris DW (1967) Carrying capacity of notched column. *Int J Solids Struct* 3:489–500
12. Okamura H, Liu HW, Chu CS, Liebowitz H (1969) A cracked column under compression. *Eng Fract Mech* 1:547–564
13. Anifantis N, Dimarogonas A (1983) Stability of columns with a single crack subjected to follower and vertical loads. *Int J Solids Struct* 19(4):281–291
14. Yavari A, Sarkani S (2001) On applications of generalised functions to the analysis of Euler–Bernoulli beam-columns with jump discontinuities. *Int J Mech Sci* 43:1543–1562
15. Li QS (2001) Buckling of multi-step cracked columns with shear deformation. *Eng Struct* 23:356–364
16. Li QS (2002) Buckling of an elastically restrained multi-step non-uniform beam with multiple cracks. *Arch Appl Mech* 72:522–535
17. Fan SC, Zheng DY (2003) Stability of a cracked Timoshenko beam column by modified Fourier series. *J Sound Vib* 264:475–484
18. Caddemi S, Caliò I (2008) Exact solution of the multi-cracked Euler–Bernoulli column. *Int J Solids Struct* 45(16): 1332–1351
19. Caddemi S, Caliò I (2012) The influence of the axial force on the vibration of the Euler–Bernoulli beam with an arbitrary number of cracks. *Arch Appl Mech* 82(6):827–839
20. Wang CY, Wang CM, Aung TM (2004) Buckling of a weakened column. *J Eng Mech ASCE* 130:1373–1376
21. Viola E, Ricci P, Aliabadi MH (2007) Free vibration analysis of axially loaded cracked Timoshenko beam structures using the dynamic stiffness method. *J Sound Vib* 304: 124–153
22. Vadillo G, Loya JA, Fernandez-Saez J (2012) First order solutions for the buckling loads of weakened Timoshenko columns. *Comput Math Appl* 64:2395–2407
23. Kelly JM (2003) Tension buckling in multilayer elastomeric bearings. *J Eng Mech ASCE* 129(12):1363–1368
24. Zapata-Medina DG, Arboleda-Monsalve LG, Aristizabal-Ochoa JD (2010) Static stability formulas of a weakened Timoshenko column: effects of shear deformations. *J Eng Mech ASCE* 136(12):1528–1536
25. Caddemi S, Caliò I, Cannizzaro F (2013) The influence of multiple cracks on tensile and compressive buckling of shear deformable beams. *Int J Solids Struct* 50:3166–3183
26. Zaccaria D, Bigoni D, Noselli G, Misseroni D (2011) Structures buckling under tensile dead load. *Proc R Soc A* 467(2130):1686–1700

27. Bigoni D, Misseroni D, Noselli G, Zaccaria D (2014) Surprising instabilities of simple elastic structures. In: Kirillov N, DE Pelinovsky (eds) *Nonlinear physical systems—spectral analysis, stability and bifurcations*. Wiley, London, pp 1–14 ISBN: 978-1-84821-420-0
28. Caddemi S, Calì I, Cannizzaro C (2013) Closed-form solutions for stepped Timoshenko beams with internal singularities and along-axis external supports. *Arch Appl Mech* 83(4):559–577
29. Colombeau JF (1984) *New generalized functions and multiplication of distribution*. North-Holland, Amsterdam
30. Hoskins RF (1979) *Generalised functions*. Ellis Horwood Limited, Chichester
31. Zemanian AH (1965) *Distribution theory and transform analysis*. McGraw-Hill, New York